

Case studies in resonance polarization and the Hanle effect

M. Landolfi

*Istituto Nazionale di Astrofisica, Osservatorio di Arcetri, Largo E.
Fermi 5, I-50125 Firenze, Italy*

E. Landi Degl’Innocenti

*Dipartimento di Astronomia e Scienza dello Spazio, Università di
Firenze, Largo E. Fermi 2, I-50125 Firenze, Italy*

Abstract. We present an overview of the scattering process by a two-level atom, aimed at clarifying how the polarization of the scattered radiation is affected by the main physical factors – atomic transition, magnetic field, depolarizing collisions, lower-level polarization, stimulated emission.

1. Introduction

The general theory of line formation in the presence of a magnetic field is based on the NLTE approach: here one has to find a consistent solution for the radiation field and for the state of matter (the atoms and ions interacting with the radiation field) at each point of the medium considered. The basic equations involved are the statistical equilibrium equations for the (non-diagonal) atomic density matrix and the radiative transfer equation for polarized radiation. The solution to the problem implies complex numerical calculations, which usually make difficult to understand the underlying physics – the role of the different processes at the atomic level.

In an attempt to clarify this role, we consider here just one of the ‘steps’ involved in the NLTE problem, that is, the behaviour of an atom under given physical conditions. In other words, we consider an atom illuminated by a given radiation field, in the presence of a given magnetic field and of given collisional rates, and we study the properties of the re-emitted radiation.

We further restrict the problem to the following: i) a two-level model atom, each level being characterized by a total angular momentum J ; in the notation $|\alpha JM\rangle$, J is the quantum number associated to angular momentum, M the magnetic quantum number associated to its projection on the quantization axis, and α is a collection of inner quantum numbers of the atomic Hamiltonian; ii) an isotropic distribution of colliding particles, able to produce depolarizing (elastic) collisions; we disregard inelastic collisions that can induce transitions between the two levels; iii) we assume the incident radiation to be frequency-independent across an interval centered at the transition frequency ν_0 and wider than the inverse lifetimes of the levels and of the Zeeman splittings produced by the magnetic field: this limitation is intrinsic to the equations used in the following.

We refer to the equations written in the formalism of spherical tensors. In this formalism, the elements of the density matrix between eigenstates of angular momentum are replaced by linear combinations of them involving a Clebsh-Gordan coefficient (or a 3- j symbol), referred to as statistical tensors,

$$\rho_Q^K(\alpha J) = \sum_{MM'} (-1)^{J-M} \sqrt{2K+1} \begin{pmatrix} J & J & K \\ M & -M' & -Q \end{pmatrix} \langle \alpha JM | \rho | \alpha JM' \rangle .$$

In particular, the $Q = 0$ components of the statistical tensors are linear combinations of *populations* of the magnetic sublevels (and ρ_0^0 is proportional to the overall population of the αJ -level), while components with non-zero Q are combinations of *coherences* between different magnetic sublevels. The statistical tensors with $K = 1$ or $K = 2$ are usually referred to as atomic orientation and alignment, respectively.

The statistical equilibrium equations for the statistical tensors of the upper and lower level, written in a reference system where the atom is at rest and with the z -axis in the magnetic field direction, read (see, e.g., Landi Degl'Innocenti 1984, 1985; Landi Degl'Innocenti, Bommier, & Sahal-Br  chot 1990)

$$\begin{aligned} \frac{d}{dt} \rho_Q^K(u) &= -2\pi i \nu_L g_u Q \rho_Q^K(u) + \sum_{K'Q'} T_A(\alpha_u J_u K Q, \alpha_\ell J_\ell K' Q') \rho_{Q'}^{K'}(\ell) \\ &\quad - \sum_{K'Q'} \left[R_E(\alpha_u J_u K Q K' Q') + R_S(\alpha_u J_u K Q K' Q') \right] \rho_{Q'}^{K'}(u) \\ &\quad - D(\alpha_u J_u K) \rho_Q^K(u) , \end{aligned}$$

$$\begin{aligned} \frac{d}{dt} \rho_Q^K(\ell) &= -2\pi i \nu_L g_\ell Q \rho_Q^K(\ell) \\ &\quad + \sum_{K'Q'} \left[T_E(\alpha_\ell J_\ell K Q, \alpha_u J_u K' Q') + T_S(\alpha_\ell J_\ell K Q, \alpha_u J_u K' Q') \right] \rho_{Q'}^{K'}(u) \\ &\quad - \sum_{K'Q'} R_A(\alpha_\ell J_\ell K Q K' Q') \rho_{Q'}^{K'}(\ell) - D(\alpha_\ell J_\ell K) \rho_Q^K(\ell) . \end{aligned}$$

The structure of the two equations is quite similar. For instance, the statistical tensors of the upper level have a positive contribution from absorption processes (rate T_A) and a negative contribution from spontaneous and stimulated emission processes (rates R_E and R_S). The first term in the right-hand side, where ν_L is the Larmor frequency and g_u the Land   factor of the upper level, is responsible for the Hanle effect. The rate D in the third line describes depolarizing collisions: it is independent of Q as a consequence of the assumed isotropy of collisions, and it is identically zero for $K = 0$ because depolarizing collisions only affect atomic polarization, not populations.

In stationary situations the time derivatives in the left-hand sides are zero and we are left with an algebraic, linear, homogeneous system of equations with zero determinant which must be supplemented with the trace equation describing the normalization of the density matrix,

$$\sqrt{2J_\ell + 1} \rho_0^0(\ell) + \sqrt{2J_u + 1} \rho_0^0(u) = 1 .$$

Once the incident radiation, the magnetic field and the collisional rates are specified, all the coefficients are known: to determine the state of the atom

simply means solving the algebraic system. The only problem with this is that, even for simple transitions (that is, low J values), we get a large number of equations. This is why it is difficult to derive any general result unless some additional approximation is introduced.

2. The unpolarized-lower-level approximation

A widely used approximation is to neglect the atomic polarization of the lower level. This is correct – by definition – for the transition ($J_\ell = 0, J_u = 1$). In general, this approximation is justified when, for the lower level, the collisional rates are much larger than the radiative rates, and this is especially true in the presence of a weak radiation field; therefore, the unpolarized-lower-level approximation also implies that stimulated emission can be neglected.

The simplification so obtained is obvious: as $R_E = A_{ul} \delta_{KK'} \delta_{QQ'}$, where A_{ul} is the Einstein coefficient for spontaneous de-excitation, in the equation for the upper level we can factor out – in stationary situations – the upper-level statistical tensors, which turn out to be proportional to the lower-level population,

$$\rho_Q^K(u) = \frac{T_A(\alpha_u J_u K Q, \alpha_\ell J_\ell 0 0)}{A_{ul} + 2\pi i \nu_L g_u Q + D(\alpha_u J_u K)} \rho_0^0(\ell). \quad (1)$$

Since the emissivity in each of the Stokes parameters depends linearly on the upper-level statistical tensors, and since the radiative rate for absorption is proportional to the radiation field tensor (which is the solid-angle average of a linear combination of the Stokes parameters of the incident radiation), we immediately obtain an analytical expression relating the emissivity (in a given direction, and at a given frequency) to the Stokes parameters of the incoming radiation.

We consider in succession 3 sub-cases: I) no collisions, no magnetic field (that is, resonance polarization); II) then we add a magnetic field, to see the modifications to resonance polarization due to the Hanle effect; III) next we look at the modifications due to depolarizing collisions.

I) Resonance polarization. The coefficient relating the upper-level statistical tensors to the population of the lower level is simply the absorption rate T_A divided by the spontaneous emission rate, that is, the Einstein coefficient A_{ul} . Substituting the expression for T_A , we can write the emissivity in the form

$$\epsilon_i(\nu, \vec{\Omega}) \propto \phi(\nu_0 - \nu) \oint \frac{d\Omega'}{4\pi} \sum_{j=0}^3 P_{ij}(\vec{\Omega}, \vec{\Omega}') S_j(\nu_0, \vec{\Omega}') \quad (i = 0, 1, 2, 3),$$

where, neglecting the width of the lower level

$$\phi(\nu_0 - \nu) = \frac{1}{\pi} \frac{\Gamma}{\Gamma^2 + (\nu_0 - \nu)^2}, \quad \Gamma = \frac{A_{ul}}{4\pi}.$$

The element (i, j) of the scattering matrix P gives the contribution of the j -th Stokes parameter of the incoming radiation to the emissivity in the i -th Stokes parameter. If we introduce the scattering angle Θ , and define the positive- Q

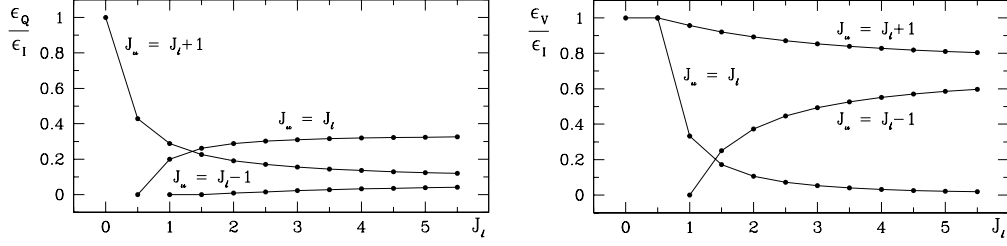


Figure 1. Fractional polarization of the scattered radiation for different transitions, calculated from Eqs.(2).

direction as the perpendicular to the scattering plane (both for the incoming and for the outgoing radiation), the matrix P takes the simple form

$$P = \begin{pmatrix} 1 - \frac{1}{4} W_2 (1 - 3 \cos^2 \Theta) & \frac{3}{4} W_2 \sin^2 \Theta & 0 & 0 \\ \frac{3}{4} W_2 \sin^2 \Theta & \frac{3}{4} W_2 (1 + \cos^2 \Theta) & 0 & 0 \\ 0 & 0 & \frac{3}{2} W_2 \cos \Theta & 0 \\ 0 & 0 & 0 & \frac{3}{2} W_1 \cos \Theta \end{pmatrix},$$

with

$$W_K = 3(2J_u + 1) \left\{ \begin{matrix} 1 & 1 & K \\ J_u & J_u & J_l \end{matrix} \right\}^2.$$

These expressions show that: i) The emissivity in each of the Stokes parameters has the same frequency dependence (a Lorentzian profile centred at the transition frequency and having a width related only to the natural width of the upper level): therefore, the fractional polarization is *frequency-independent*. ii) For an unpolarized incident beam, the U Stokes parameter of the scattered radiation is zero and the Q Stokes parameter is positive: thus the scattered linear polarization is always *perpendicular* to the scattering plane. iii) The matrix P depends both on the *scattering geometry* (the angle Θ) and on the *atomic transition*, through the J quantum numbers of the upper and lower level. iv) The W_2 coefficient is related to *linear* polarization, the W_1 coefficient to *circular* polarization; note that circular polarization can be present in the scattered radiation only if some circular polarization is already present in the incident radiation.

To quantify the dependence of scattered polarization on the atomic transition, we can consider two extreme situations. If the incident radiation is an unpolarized beam, the fractional linear polarization is maximum for $\Theta = 90^\circ$; if the incident radiation is a totally circularly polarized beam, the fractional circular polarization is maximum for $\Theta = 0^\circ$. Such polarizations are given by

$$\frac{\epsilon_Q}{\epsilon_I} = \frac{3W_2}{4 - W_2}, \quad \frac{\epsilon_V}{\epsilon_I} = \frac{3W_1}{2 + W_2}, \quad (2)$$

and are plotted in Fig.1 (left and right panel, respectively) as functions of

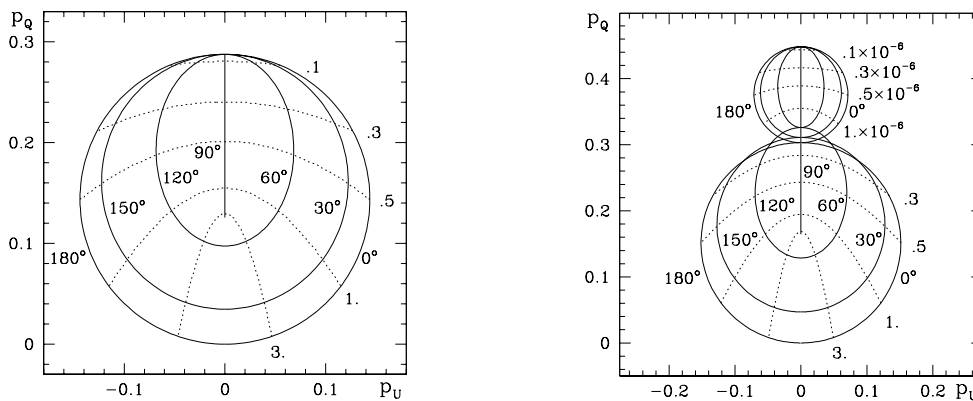


Figure 2. Hanle diagrams for the transition ($J_\ell = 1, J_u = 2$). Left: assuming the lower level to be unpolarized. Right: allowing for lower-level polarization.

J_ℓ , for transitions with $\Delta J \equiv J_u - J_\ell = 0, \pm 1$. We see that the ‘polarizing efficiency’ depends in a complicated way on the atomic transition: in the case on the left, only the transition $(0, 1)$ has efficiency unity; all the others have an efficiency below 0.5. For large J values, the transitions with $\Delta J = 0$ are the most efficient. In the case on the right, there are 3 transitions with efficiency unity: $(0, 1)$, $(1/2, 3/2)$, and $(1/2, 1/2)$. The efficiency remains large for all transitions with $\Delta J = 1$, followed by those with $\Delta J = -1$, which are the least efficient with respect to linear polarization.

II) Resonance polarization in the presence of a magnetic field, or the Hanle effect. Now we have an additional term in the denominator (see Eq.(1)): the upper-level statistical tensors are the same as in the zero-field case (where it is understood that the same radiation field and reference system is used), divided by $(1 + iQH)$, where i is the imaginary unit and the dimensionless quantity H is the ratio of the Larmor frequency (times the Landé factor of the upper level) to the Einstein coefficient for spontaneous emission,

$$\rho_Q^K(u) = \frac{[\rho_Q^K(u)]_{B=0}}{1 + iQH}, \quad H = \frac{2\pi \nu_L g_u}{A_{ul}}. \quad (3)$$

This expression contains the basic features of the Hanle effect: it shows that the $Q = 0$ components of the statistical tensors (hence the populations of the magnetic sublevels) are *unaffected* by the magnetic field, while coherences are both *reduced* and *de-phased*. The maximum sensitivity for these phenomena is to be expected for H values close to unity. It is well-known the lucky circumstance that for typical values of the Einstein coefficient and of the Landé factor, H unity means a field strength of about 10 G: this led to the recent ‘re-discovery’ of the Hanle effect for astrophysical applications, mainly to solar prominences.

The Hanle effect is typically visualized by considering the 90° scattering of an unpolarized radiation beam, with a magnetic field perpendicular to the beam and making some angle β with the line of sight, and by plotting, one against the

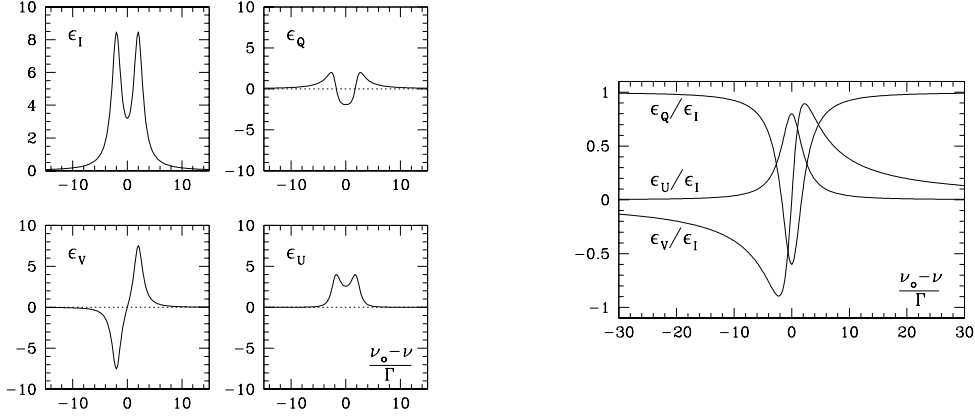


Figure 3. The emissivity (in arbitrary units) of the transition ($J_\ell = 0, J_u = 1$) corresponding to the 90° scattering of an unpolarized incident beam. The profiles are plotted against reduced frequency. The magnetic field is characterized by $H = 1, \beta = 0^\circ$.

other, the frequency-integrated fractional emissivities in Q and U ,

$$p_Q = \int \epsilon_Q d\nu / \int \epsilon_I d\nu, \quad p_U = \int \epsilon_U d\nu / \int \epsilon_I d\nu,$$

while varying the field modulus and the angle β .

An example for the transition ($J_\ell = 1, J_u = 2$) is shown in Fig.2 (left). Full lines correspond to constant β , dashed lines to constant field modulus: these are labelled by the value of the parameter H . For zero field we have only Q (polarization perpendicular to the scattering plane), with the value corresponding to ‘pure’ resonance polarization – something less than 0.3. When H is increased, coherences are reduced and de-phased, so we get some U ; which again vanishes for sufficiently large H . The diagram is degenerate for opposite β values, while inversion of the magnetic field’s direction yields the same Q and opposite U .

But when a magnetic field is present, besides the reduction and de-phasing of the upper-level statistical tensors, there is also a *Zeeman splitting* of the magnetic sublevels, whose effects show up when we look at the profiles of the emissivity rather than the frequency-integrated emissivity.

An example is shown in Fig.3. The I, Q , and U profiles originate from the combined effect of Zeeman splitting and atomic alignment, whereas the V profile is due only to Zeeman splitting, because an incident unpolarized beam cannot induce atomic orientation. It is especially interesting to look at the profiles of fractional polarization (Fig.3 right). We see that in the far wings, U/I and V/I tend to zero, but Q/I tends to unity, which is the value of resonance polarization (zero magnetic field) for the transition ($J_\ell = 0, J_u = 1$). In fact it can be proved that, for any transition, the Hanle effect vanishes in the far wings.

III) Consider the effect of depolarizing collisions. Now we have a third term in the denominator (see Eq.(1)), and besides the ‘Hanle parameter’ H we can introduce a new dimensionless quantity: the ratio of the collisional rate $D(\alpha_u J_u K)$ to the Einstein coefficient $A_{u\ell}$, that may be regarded as the ‘effective’

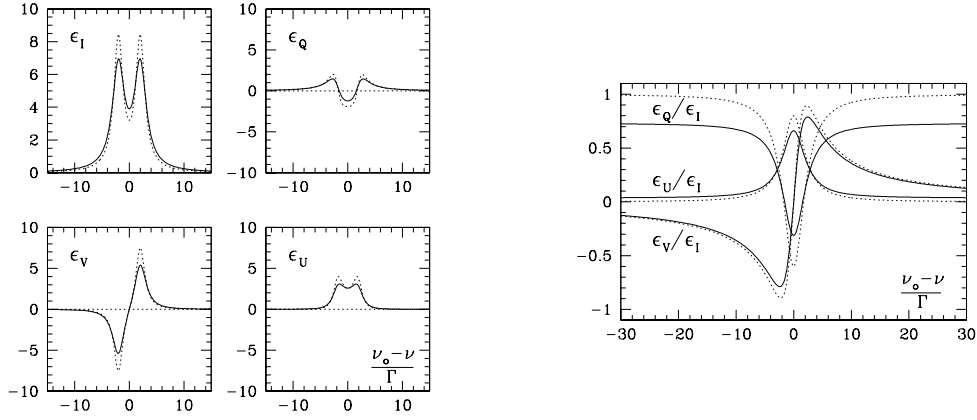


Figure 4. Effect of depolarizing collisions on the profiles of Fig.3.

number of depolarizing collisions (for the statistical tensors of rank K) taking place during the lifetime of the excited level,

$$\rho_Q^K(u) = \frac{[\rho_Q^K(u)]_{B=0, D=0}}{1 + iQH + \delta_u(K)}, \quad \delta_u(K) = \frac{D(\alpha_u J_u K)}{A_{ul}}. \quad (4)$$

The new term $\delta_u(K)$ is real, so the net effect is a *reduction* of polarization (atomic polarization, and therefore polarization of the scattered light). Moreover, the profiles of the emissivity will be broadened by the addition of a collisional damping constant Γ_c .

Figure 4 shows how the profiles of Fig.3 (dashed curves) are changed by the presence of depolarizing collisions such that the parameter $\delta_u(2)$ is 0.2 and the ratio of collisional to radiative damping constant is appropriate to Van der Waals-type interactions ($\Gamma_c/\Gamma = \delta_u(2) \times 5/3$). The effect is more obvious on fractional polarization, which is reduced at every single frequency; especially obvious is the effect on the asymptotic value of Q/I .

3. The effects of lower-level polarization

Let's see how things change if we allow for the presence of lower-level atomic polarization. Now there is no short cut: we must solve the coupled system of equations for the upper and lower level.

Consider first the non-magnetic case (resonance polarization). In general, besides the quantity $\delta_u(K)$ of Eq.(4) it is necessary to introduce two additional (dimensionless) parameters: the ratio between the total absorption and spontaneous emission probability – or, equivalently, the number of photons per mode at the transition frequency averaged over the solid angle,

$$\bar{n} = \frac{(2J_\ell + 1) B_{\ell u} J_0^0(\nu_0)}{(2J_u + 1) A_{ul}} = \frac{c^2}{2h\nu_0^3} J_0^0(\nu_0),$$

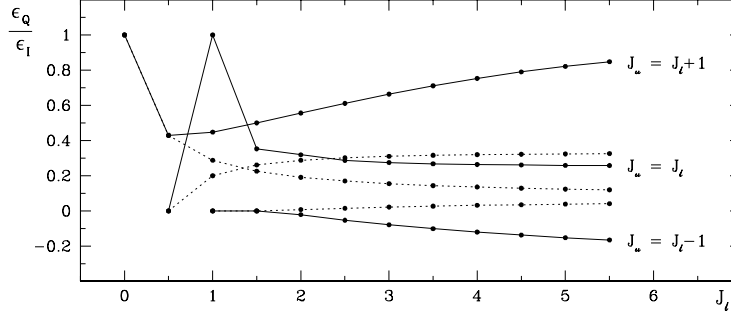


Figure 5. The effect of lower-level polarization on the fractional linear polarization of the scattered radiation, for different transitions.

and the ratio of the collisional rate for the lower level to the absorption rate,

$$\delta_\ell(K) = \frac{D(\alpha_\ell J_\ell K)}{B_{lu} J_0^0(\nu_0)} = \frac{2J_\ell + 1}{2J_u + 1} \frac{D(\alpha_\ell J_\ell K)}{A_{u\ell}} \frac{1}{\bar{n}}.$$

To get a general idea of the effects of lower-level polarization, we may refer again to the 90° scattering of an unpolarized radiation beam and look at the polarization of the scattered radiation. Assuming $\bar{n} \ll 1$ (no stimulated emission) and neglecting collisions ($\delta_u(K) = \delta_\ell(K) = 0$), we obtain the results of Fig.5. The dashed curves correspond to the unpolarized-lower-level approximation (cf. Fig.1 left), the solid curves take lower-level polarization into account. We see that there is a large increase of polarization for transitions with $\Delta J = 1$, a small effect for transitions with $\Delta J = 0$ – with the only exception of the transition (1,1) – and something intermediate for $\Delta J = -1$: here the most interesting aspect is that Q/I is negative, thus the polarization is *parallel* to the scattering plane.

Hanle effect with lower-level polarization. The main point is this one: under the unpolarized-lower-level approximation, the Hanle effect is basically described by the parameter H of Eq.(3), the ratio between the Larmor frequency and the rate for spontaneous emission; now we should expect that the corresponding parameter for the *lower* level, i.e., the ratio between the Larmor frequency and the *absorption* rate, also plays a role. And we should expect that the ratio of the typical field intensities for lower- and upper-level depolarization be approximately the same as the ratio of the two rates, namely the average number of photons per mode \bar{n} .

Figure 2 (right) shows the Hanle diagram for the transition ($J_\ell = 1, J_u = 2$), relative to the collisionless case and to the usual scattering geometry (90° , with an unpolarized incident beam and a magnetic field perpendicular to the beam). The parameter \bar{n} is very small (10^{-6}), so we have two clearly distinct regimes: the lower, characterized by H values of order unity, is the ‘ordinary’ Hanle effect and corresponds to the destruction of upper-level coherences; the upper, characterized by H values of order 10^{-6} , is referred to as lower-level Hanle effect and corresponds to the destruction of lower-level coherences.

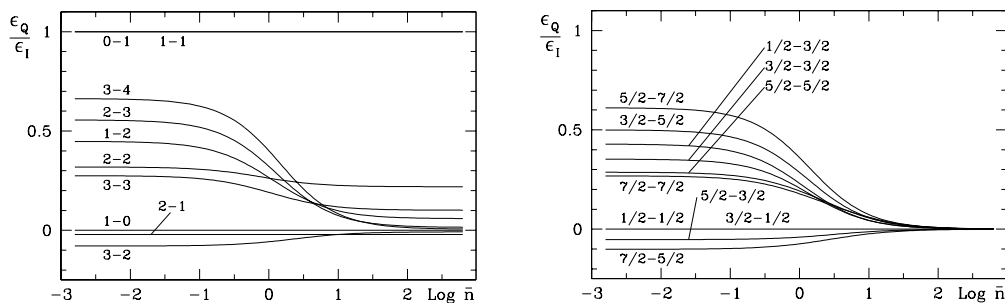


Figure 6. Fractional linear polarization of the scattered radiation for different transitions ($J_\ell - J_u$), as a function of the beam intensity expressed in terms of the average number of photons per mode \bar{n} .

4. The effects of stimulated emission

Finally, a look at the effects of stimulated emission. Now lower-level polarization *must* be taken into account, because when the radiation field is not weak (that is, \bar{n} is comparable to unity) it doesn't make sense to invoke depolarizing collisions in the lower level only: the radiative lifetimes of the upper and lower level become comparable, and if collisions are so strong to destroy lower-level polarization, they will also destroy upper-level polarization.

Figure 6 shows what happens to resonance polarization when the radiation field intensity is increased. The figure refers to the usual 90° scattering geometry, an incident unpolarized beam, no collisions, no magnetic field. For some transitions with low J values the scattered polarization is unaffected by the field intensity: (0, 1) and (1, 1) with polarization unity; (2, 1) with a small negative polarization; (1/2, 1/2) and (3/2, 1/2) with polarization zero. But for all the others, the polarization *decreases* (in absolute value) with increasing field intensity.

This can be understood if we consider that atomic polarization arises from the fact that, in an anisotropic environment, transitions between certain magnetic sublevels of the upper and lower level are more efficient than the others in absorbing radiation, and this produces a population unbalance; but when stimulated emission is important, just the *same* transitions are more efficient in *emitting* radiation, so the unbalance is reduced.

We have grouped the transitions according not to the ΔJ value, but to integer and half-integer J , to point out a curious feature: if J is half-integer, the polarization tends to zero, otherwise to a non-zero, transition-dependent value.

When we add a magnetic field (Hanle effect in the presence of a radiation field of increasing intensity), the main effect to be expected is a *mixing of the two regimes* of the 'ordinary' and 'lower-level' Hanle effect, because the radiative lifetimes of the upper and lower level tend to become comparable.

This is illustrated in Fig.7, which shows how the Hanle diagram of Fig.2 (right) changes when the intensity of the incoming beam is increased. The two distinct regimes of Fig.2 (right), where $\bar{n} = 10^{-6}$, are partly mixed for $\bar{n} = 0.03$

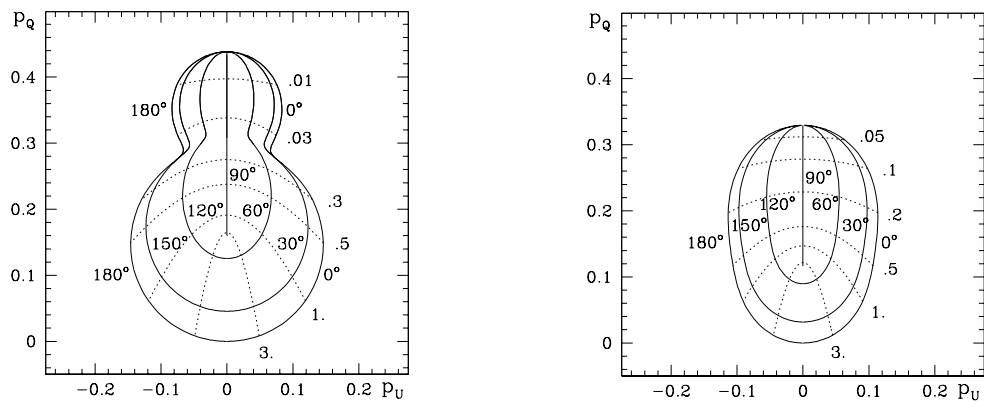


Figure 7. Hanle diagrams for the transition ($J_\ell = 1, J_u = 2$) corresponding to different intensities of the incident radiation beam: $\bar{n} = 0.03$ (left) and $\bar{n} = 0.5$ (right).

and completely merged for $\bar{n} = 0.5$. In the panel on the right the double-lobe shape of the diagram has completely disappeared. At the same time the zero-field polarization is smaller, consistently with the results of Fig.6 (left).

References

- Landi Degl'Innocenti, E. 1984, *Solar Phys.*, 91, 1
 Landi Degl'Innocenti, E. 1985, *Solar Phys.*, 102, 1
 Landi Degl'Innocenti, E. , Bommier, V., & Sahal-Br echot, S. 1990, *A&A*, 235, 459

Discussion

S. SAHAL-BRECHOT: If collisional line broadening includes depolarizing collisional cross sections, it also includes other contributions such as elastic cross sections which do not depolarize. Collisional line broadening also includes an interference term between the upper and lower level. Do you take into account elastic terms in your expressions for the collisional broadening of the levels (lines)?

M. LANDOLFI: In the example of Fig.4 we neglected the interference term, as well as the broadening of the lower level due to elastic collisions: we used an approximate expression for the collisional broadening valid for dipole-dipole interactions. However, the precise value of the collisional damping constant does not change the qualitative effect shown in the figure, particularly the fact that, when collisions are present, the Hanle effect does *not* vanish in the far wings of the line.